

The role of material composition in the construction of viscoelastic master  
curves: silica-filler network effects

By S. Maghami<sup>\*a</sup>, W. K. Dierkes<sup>a</sup>, T. V. Tolpekina<sup>b</sup>, S. M. Schultz<sup>b</sup>, J. W. M.  
Noordermeer<sup>a</sup>

<sup>a</sup>University of Twente, Elastomer Technology and Engineering,  
7500 AE Enschede, the Netherlands

<sup>b</sup>ApolloVredestein BV,  
7500 AA Enschede, the Netherlands

Presented at the Fall 180th Technical Meeting of the  
Rubber Division of the American Chemical Society, Inc.  
Cleveland, Ohio  
October 11-13, 2011

ISSN: 1547-1977

\*speaker

## ABSTRACT

One of the important aspects in the development of new tire compounds is the correlation between the dynamic mechanical properties of the rubber, measured on laboratory scale, and the actual tire performance. The measuring protocol for dynamic mechanical properties with high precision and good correlation with tire properties is therefore of main concern. In order to predict wet traction, the viscoelastic behavior of the rubber materials at high frequencies (in the MHz range) need to be known. Viscoelastic master curves derived from time-temperature superposition can be used to describe the properties of the materials over a wide frequency range.

In this paper, the construction of master curves for tread compounds filled with different amounts of silica is discussed. From the vertical shifts as a function of temperature activation energies are derived which apparently are in the linear response region by fulfilling the Kramers-Kronig relations, and their values correspond to physical phenomenon as the underlying principle.

Strain sweep viscoelastic measurements, per definition outside the linear region, lead to much higher activation energies. Because the deformation strains employed for these strain sweep measurements are more realistic for wet traction or skidding phenomena it is concluded that the value of the above measurements in the linear region to predict traction is only limited or a first but still important indication.

## INTRODUCTION

A tire interacts with the hard road surface by deforming under load, thereby generating the forces needed for traction, cornering, acceleration and braking. It also provides increased cushioning for driving comfort. Traction, especially under wet conditions, is the most important tire property from a safety point of view. Traction is directly related to energy lost in each deformation cycle: each point in the tire passes through a stress-strain cycle once every rotation<sup>1-7</sup>. Due to the viscoelastic nature of the rubber compound, the deformation leads to energy loss in the form of heat in each cycle. Although it has been stated that the tread pattern and the roughness of the road surface are as important as the loss properties of the tire tread material in determining the skid properties, the current trend is basically to concentrate on the latter for improvements in performance.

In order to predict wet traction, the viscoelastic properties of the rubber materials at high frequencies, in the megahertz (MHz) range, should be measured. Heinrich et al.<sup>8-10</sup> have done investigations on the wet skid behavior of different polymers and concluded that neither the glass transition of the polymers alone nor their plateau modulus  $G_N^0$  gives good correlation with wet skid resistance (WSR). A good correlation is only found when relating the WSR to the viscoelastic behavior of the elastomers in the transition region which is typically in the range of 1 kHz- 1 MHz.

In practice, measuring dynamic properties is limited by the accessible frequency range of the instrument. However, the modulus at high frequencies is available via the time-temperature superposition principle. According to this principle, the effect of changing the temperature is the same as applying a shift factor  $a_T$  to the time scale. The time-temperature superposition for polymeric materials was proposed by Williams, Landel and Ferry in 1955<sup>11,12</sup> and is generally

referred to as the WLF principle. According to this principle, the horizontal shift factor  $a_T$  is given by:

$$\log(a_T) = \frac{-C_1(T - T_{ref})}{C_2 + (T - T_{ref})} \quad (1)$$
$$T_g < T < T_g + 100^\circ C$$

where  $T$  is temperature and  $T_g$  is the glass transition temperature. The constants  $C_1$  and  $C_2$  vary with the choice of the reference temperature  $T_{ref}$ . If the glass transition temperature is taken as the reference temperature, the two constants have almost universal values for many high diene rubbers:  $C_1 = 17.4$  and  $C_2 = 51.6$ . If  $T_g + 50^\circ C$  is taken as  $T_{ref}$ , then  $C_1 = 8.86$  and  $C_2 = 101.6$ . These values only differ slightly from one polymer system to the other.

The WLF principle has been proven to work well for polymers in their molten state, irrespective of whether they are crosslinked or not, as it is based on the free-volume concept<sup>12,13</sup>. If fillers are added to these polymers, and most particularly reinforcing fillers like carbon black and silica, the WLF-principle does not work properly anymore. Some overlapping of the curves is then seen in the lower frequency range<sup>14-16</sup>. The reason is the additional effect of polymer–filler and even more so filler–filler interactions. The latter is commonly designated as the “filler network”, for which the free-volume concept obviously does not apply. The overlapping in the low frequency region (or v.v. high temperature region) indicates that the filler network dominates here the dynamic mechanical properties of the filler-rubber composite as the rubber matrix is softer<sup>14</sup>. In order to eliminate these overlapping and receive a proper master curve, vertical shifting is necessary.

The filler network manifests itself in various ways, like the need for an additional vertical shift in the creation of dynamic mechanical mastercurves over the common vertical shift accounting for temperature corresponding density differences, in the non-linear Mullins effect<sup>17-</sup>

<sup>19</sup> and the Payne effect <sup>20,21</sup>. An all-inclusive theory relating all these different elements of the behaviour of the filler network does not exist as yet. But all these effects are based on physical principles and therefore should basically respond to temperature variations according to corresponding relatively low activation energies compared to chemically based mechanisms.

The construction of master curves for carbon black and silica reinforced rubbers has been the subject of several experimental as well as theoretical papers already <sup>14-16</sup>. It is commonly understood that a silica filler-network is even stronger than a carbon black network <sup>21,22</sup>. In the present paper, the construction of master curves based on the dynamic mechanical experiments for a tire tread rubber compound with varied silica filler-loading is discussed. In addition, strain sweep measurements detailing the Payne effect are presented. Activation energies will be derived from the temperature dependence of the vertical shift in the creation of master curves, resp. of the Payne effect and correlated with the material composition.

## **EXPERIMENTAL**

### **MATERIALS AND COMPOUND PREPARATION**

Blends of oil-extended solution styrene-butadiene rubber (S-SBR) and high-cis polybutadiene (BR) with a weight ratio of 70/30 were used in this study. Compounds have been prepared based on the formulations given in Table I. In the acronym used, 3 stands for 30 phr of BR and 7 for 70 phr of SSBR. S indicates the silica filler and the last number shows the amount of silica: 6 for 60, 7 for 70 and 8 for 80 phr silica. A highly dispersible silica was used as reinforcing filler. The amount of silica was varied between 60 and 80 phr. The amount of coupling agent has been adjusted according to the amount of silica to maintain the same weight ratio. The rest of the ingredients and suppliers are listed in Table I.

The compounds were prepared in a 350 ml Brabender 350S internal mixer Operating at 100 rpm with a filling factor 0.7. The total mixing time was 9 minutes while the dump temperature was adjusted to approximately 155 °C (by changing the initial temperature). The samples were cured in a Wickert press WLP 1600 at 160 °C to sheets with a thickness of 1.5 mm according to their  $t_{90}$  optimum vulcanization time as determined in a rubber process analyzer RPA 2000.

## **MEASUREMENTS**

Dynamic mechanical analyses were performed in the shear and tension mode in a Metravib DMA2000 dynamic spectrometer. The samples were cut from the cured sheets of the rubber compounds. For producing master curves, time-temperature superposition measurements were performed at different temperatures between -20 °C and 80 °C in steps of five degrees at a dynamic strain of 0.1% and the frequency range of 1-200 Hz. The glass transition temperatures were obtained from temperature sweep measurements in tension mode at a frequency of 1 Hz and dynamic strain of 0.1%. Strain sweep measurements were performed at 10 Hz at different temperatures from 60 to 80 °C.

## **RESULTS AND DISCUSSION**

### **MASTER CURVE VIA TIME-TEMPERATURE SUPERPOSITION MEASUREMENTS:**

#### **HORIZONTAL SHIFT**

Time-temperature superposition measurements have been performed on the compounds. It is basically a frequency sweep at different temperatures for a specified dynamic strain. The raw data for the storage modulus of compound 37S7 were presented in Figure 1 as an example.

To produce master curves for these filler reinforced compounds, first a horizontal shift is done along the frequency axis. The WLF equation has been used to calculate the horizontal shift factor  $a_T$  according to equation (1).  $T_g+50$  °C and the corresponding universal constants were chosen as reference temperature and  $C_1$  and  $C_2$ , respectively. The  $T_g$  values for different compounds filled with different amount of filler were almost the same:  $-49.5\pm 1$  °C. Figure 2 shows the storage modulus after applying the horizontal shifting for the 37S7 sample. The master curve is not smooth and some overlapping of the curves at the low frequency region occurs. The physical origin of this overlapping is the superposition of two relaxation processes, the one of the polymer matrix and that of the filler network<sup>23</sup>.

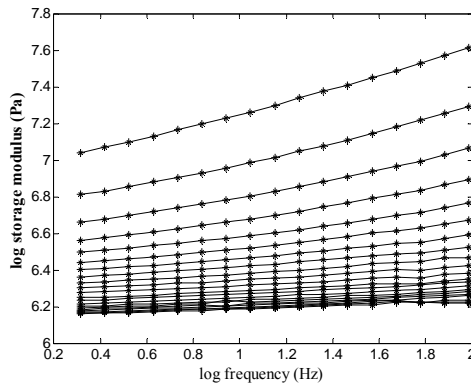


FIG. 1. - Storage modulus data for compound 37S7 derived from frequency sweep measurements performed at different temperatures between -20 °C and 80 °C in steps of five degrees at a dynamic strain of 0.1%.

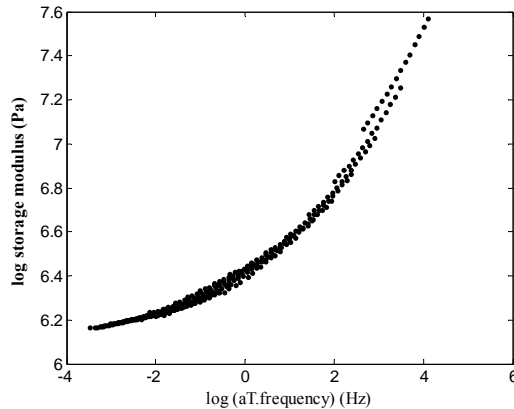


FIG. 2. - Storage modulus for 37S7 after horizontal shifting along the frequency axis,  $T_{ref}= 0$  °C.

## VERTICAL SHIFT

In order to obtain a proper master curve, vertical shifts are needed to be applied. For unfilled, non-reinforced polymers the vertical shift is commonly applied to account for the density-change of the polymers with temperature. However, because the filler network greatly overrules these polymer effects, it is common to just include these in the vertical shifting without further detailing. The vertical shifting was done numerically by a MATLAB program. During vertical shifting, the curve for the reference temperature were kept unchanged and the other isothermals shifted vertically by respective vertical shift factors  $b_T$ .

As an example, the storage modulus  $G'$  master curve after horizontal and vertical shifting for the 37S7 sample is shown in Figure 3. A nice smooth curve is obtained in this manner.

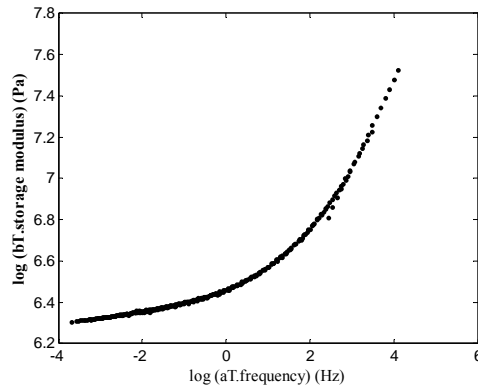


FIG.3. - Storage modulus master curve for 37S7,  $T_{ref} = 0$  °C.

Figures 4, 5 and 6 show the master curves for the storage modulus  $G'$ , the loss modulus  $G''$  and the loss tangent  $\tan\delta$  of the three different compounds.

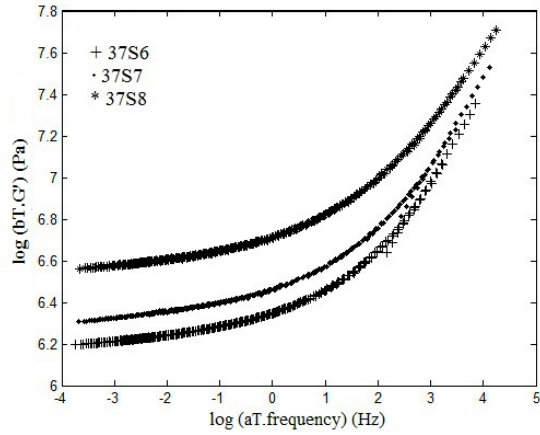


FIG. 4. - Storage modulus master curve for the different compounds.

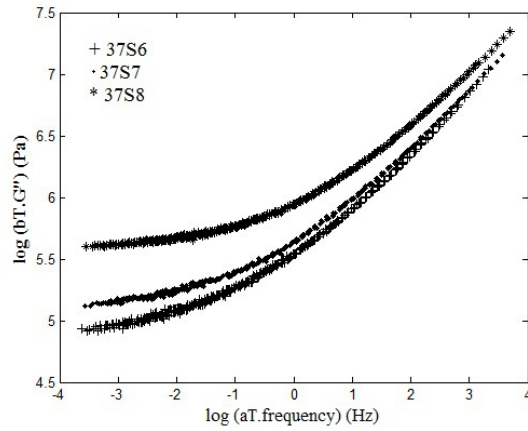


FIG. 5. - Loss modulus master curve for the different compounds.

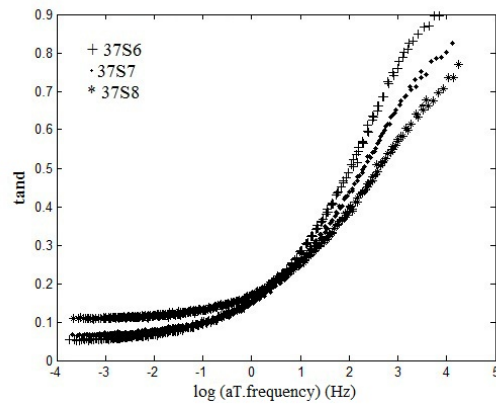


FIG. 6. - Loss tangent master curve for the different compounds.

By increasing the amount of silica filler from 60 to 80 phr, the storage and loss moduli increase. For the loss tangent  $\tan\delta$ , a crossover is observed, where in the high frequency region, the lowest filler loading gives the highest  $\tan\delta$ , but at low frequencies the order is inverted.

It has been stated before that in the high frequency (low temperature) region, unreinforced gum rubber performs best in terms of WSR. In this region, the transition zone, the polymer chains themselves are responsible for the energy dissipation<sup>24</sup>. By introduction of fillers, the fraction of free polymer chains decreases due to the fact that the polymers near to the filler surface are partly immobilized and act as filler rather than polymer: the occluded rubber concept and/or the concept of a glassy shell around the filler particle<sup>15,25-27</sup>. Whether it is a real glassy shell or a greatly reduced mobility of the polymer chains attached to the filler particles, in either case it results in decreased damping in the transition zone and consequently decreased  $\tan\delta$ .

In the low frequency region, the order in  $\tan\delta$  is reversed: the lower the filler content, the lower the  $\tan\delta$ . At a low frequency, when the polymer is largely outside the transition zone, the major source for energy dissipation is the breakdown and reformation of the filler network. Therefore, a lower  $\tan\delta$  is expected for 37S6 for which the filler network is less developed. It is clear that the filler effect at different temperatures or frequency regions is governed by different mechanisms.

In Figure 7, the resulting vertical shift factors for the storage modulus for different samples are plotted versus reciprocal temperature:  $1/T$ . A nearly linear correlation with inverse temperature well above the glass transition temperature is obtained, as indicated by the lines inserted in the figure. The slopes of these curves can be interpreted as activation energy of the filler network:  $E_a$ . Various authors have stated that this activation energy is related to the

temperature dependency of glassy shells around the filler particles<sup>14,15,23,26</sup>. The values of the activation energies for both storage and loss modulus are summarized in Table II.

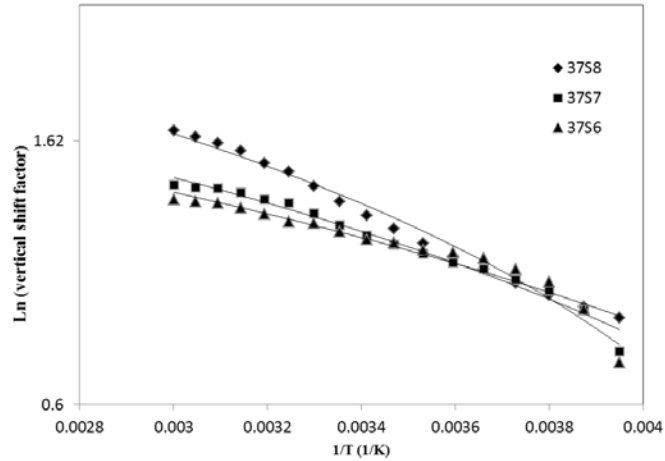


FIG. 7. - Vertical shift factor from  $G'$  vs.  $1/T$  at temperatures higher than  $T_{ref}$ .

In the linear response region, both storage and loss modulus obey the Kramers-Kronig relations<sup>28-30</sup> as the values of the activation energies derived from both are practically the same<sup>14</sup>. The differences between the two values of the activation energy are within the error margins of the measurements and calculations.

### STRAIN SWEEP MEASUREMENTS

In order to compare the behavior of the filler network in large deformations or in the non-linear region, strain sweep measurements at different temperatures from 60 to 80 °C were performed. The results of these measurements for the 37S8 sample are shown in Figures 8 and 9 for the storage and loss moduli, respectively.

The decrease in elastic modulus upon increasing the strain amplitude, the Payne effect, is commonly related to the filler-filler linkages which are broken under strain. The short-distance forces between filler particles decrease strongly from low strain to high strain values. The

breakdown of the filler network by increasing strain amplitude would also release the occluded rubber so that the effective filler volume fraction and hence the modulus decrease<sup>31</sup>. For this reason the Payne effect is being used as a measure of filler networking originating from filler-filler interaction as well as filler-polymer interaction, particularly for silica loaded rubber compounds.

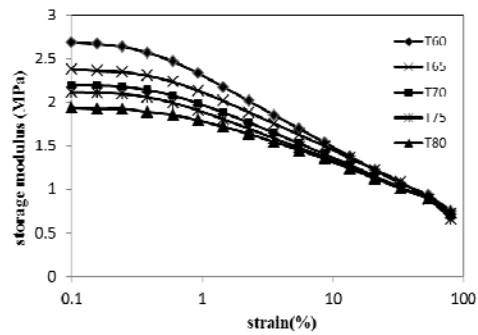


FIG. 8. - Variation of storage modulus with strain at different temperatures from 60 to 80 °C for compound 37S8.

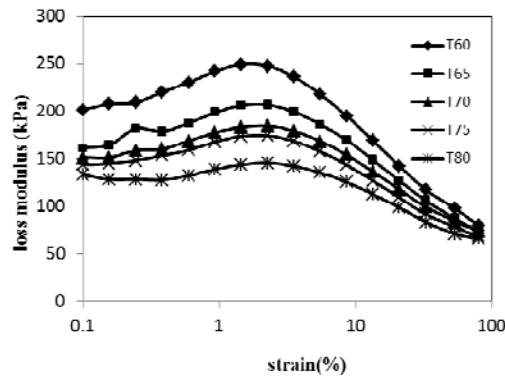


FIG. 9. - Variation of loss modulus with strain at different temperatures from 60 to 80 °C for compound 37S8.

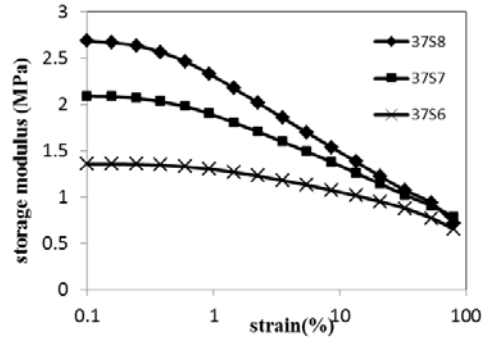


FIG. 10. - Effect of filler loading on the change of the storage modulus with strain at 60 °C.

As seen in Figure 8, the storage modulus at low amplitudes  $G'_0$  decreases with temperature, whereas the storage modulus at high amplitudes  $G'_\infty$  remains more or less constant. Similarly, in Figure 9 the loss modulus shows a temperature dependence for low strain which more or less vanishes at larger strain amplitudes. The peaks in the loss modulus vs. strain amplitude correspond to the strains where the strongest decrease in storage modulus is observed. Figure 10 shows the dependence of the Payne effect in storage modulus for different silica filler loadings, obviously being the more for higher loading. And strain, for high strain the effect of the amount of filler loading practically vanishes.

The difference between the low strain (0.1%) and high strain (80%) storage modulus, as a measure of the Payne effect, as dependent on temperature can now be used to establish an alternative Arrhenius type activation energy for the silica filler network<sup>26,27,32,33</sup>. Figure 11 gives an example for the 80 phr-loaded compound, where the natural logarithm of this Payne effect for the storage modulus is plotted against reciprocal temperature. Making use of least square fitting a straight line is drawn through the points in the figure, of which the slope gives the activation energy. This can be applied for the loss modulus as well. The activation energies derived from

both, storage and loss moduli, are summarized in Table II. The goodness of fit is shown by the  $R^2$  values, which are reasonably acceptable.

The activation energies are not the same for loss and storage moduli which is pointing to the fact that these Payne effect measurements are per definition outside the linear region. By increasing the amount of filler, the activation energies increase again, similar to what was observed in the linear region due to more pronounced filler network.

The higher activation energy in case of loss modulus can be attributed to the fact that loss modulus is correlated to the filler-filler contacts which undergo break down and reformation during the dynamic oscillation. Whereas storage modulus is related to virgin, intact filler-filler bonds<sup>14,16</sup>.

### **COMPARISON BETWEEN THE DIFFERENT METHODS**

In order to compare the previous results, the activation energies derived from both methods, the vertical shift factor and strain sweep measurements, are shown in Figure 12. By increasing the filler loading all the activation energies increase. The values of the activation energies are much higher for the results derived from the Payne effect measurements compared to those derived from the vertical shifting.

Fritzsche et al.<sup>15</sup> have done similar measurements on carbon black filled S-SBR samples and reported similar results. They concluded that in the activation energy derived from the vertical shift, the temperature dependence of filler-filler bonds plays the main role, while the dynamics on the surface of the filler is basically neglected. Therefore the values of activation energies from the vertical shift factors are lower.

Typical activation energies for physically based mechanisms are of the order of 10 (kJ/mol), whereas chemically based processes are of the order of 60-80 (kJ/mol). Along with this

reasoning the activation energies obtained from the vertical shifting exercise point at phenomena which are essentially still physical of origin.

The much higher activation energies derived from the Payne effects, but still closer to the physical than to the chemical based processes, indicate that the viscoelastic response of the compounds at such high strains cannot simply be considered as reversible physical phenomena. There is more involved than reversible rearrangement of the filler-network, or v.v. reversible chain-rearrangement of the crosslinked polymer network. The amounts of energy loss in case of the Payne-effect related large deformations are substantial because of irreversible effects, whether physical or maybe even partly chemical of nature.

The present study was triggered by the need to predict WSR of tires from viscoelastic data of rubber materials measured on laboratory scale equipment. The question may now be raised how large the deformations are of in particular the tire tread compounds during skidding or acceleration traction. Though opinions differ <sup>34-36</sup> the 7 – 8 % strain is more physically reasonable than 0.1 % strain. It implicitly puts a limit to the value of viscoelastic master curves for WSR-simulation of tire compounds. Equipment which can measure at such high deformations and high frequencies do not exist, resp. it may be questioned whether such machines are feasible from a construction standpoint. For the moment, tire designers have to make with the limited means available to combine the results from viscoelastic master curves for small deformations with separate observations on e.g. Payne effects for large deformations and make the best estimate on basis of both.

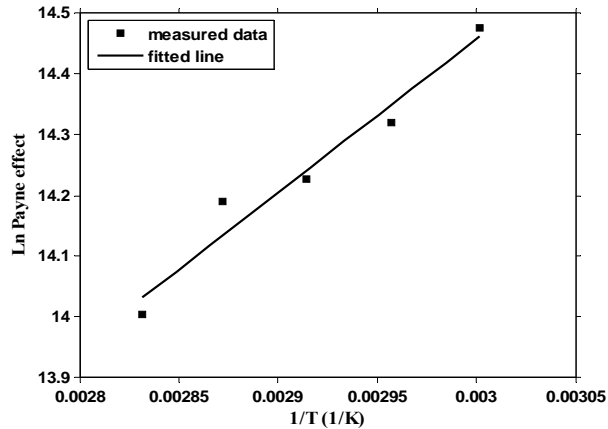


FIG. 11. - Logarithmic magnitude of storage modulus Payne effect as a function of reciprocal temperature  $1/T$  for compound 37S8.

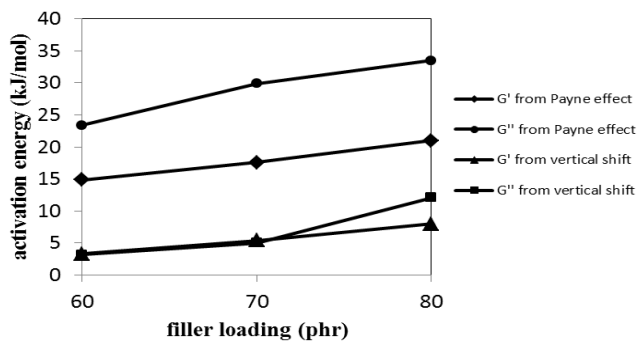


FIG 12. - Activation energies derived from the Payne effect and vertical shift factor for both  $G'$  and  $G''$  versus silica filler loading.

## CONCLUSIONS

In order to predict wet skid performance of tire tread compounds, their viscoelastic properties at very high frequencies, in the MHz range and at high deformations need to be determined. However, it is practically not possible to perform such measurements on current dynamic mechanical spectrometers. Most commonly the construction of master curves on basis of the WLF principle is then employed for small strain values in the linear region where the WLF principle is valid.

To produce a proper master curve for a silica-reinforced tire tread compound, both horizontal and vertical shifting need to be applied for the time-temperature superposition. The horizontal shift is based on the WLF principle, making use of the  $T_{ref}$  vs.  $T_g$  somewhat to compensate for the small  $T_g$ -shift with different filler loadings. The vertical shift can be considered as a thermally governed process related to the filler particles as they interact with each other (filler network), and as they are connected to the polymer chains (the filler-polymer interaction). The vertical shift factors for three tire tread compounds with resp. 60, 70 and 80 phr silica filling, show Arrhenius type behavior when plotted against  $1/T$  for the high temperature or v.v. low frequency range of the master curve. In the high frequency or v.v. low temperature region of the master curve, which is considered to be representative for the wet skid performance of tires, the loss tangent value decreases with an increase in the amount of filler. It indicates that the presence of filler negatively influences the damping properties of the polymer network. The activation energies derived from the vertical shift factors for both the storage moduli  $G'$  and the loss moduli  $G''$  at strain deformation of 0.1% are almost equal, and in the range of physical processes. It also means that the Kramers –Kronig relations are fulfilled in this linear response region.

In the high frequency region of the master curve, which is believed to be responsible for the wet skid performance of tires, the loss tangent value decreases with an increase in the amount of filler. This can be explained by the occluded rubber concept. In the transition zone polymer chains are responsible for the energy loss. By introduction of fillers some parts of polymer near the filler surface get immobilized so the energy loss decreases.

Strain sweep measurements performed at different temperatures with strains between 0.1 and 100% on the same three compounds give the activation energies which are 3-5 times higher

than for the vertical shifting operation. Furthermore, the values derived from the loss modulus  $G''$  are much higher than those derived from the storage modulus  $G'$ . As mentioned before, this has been related to different behavior of storage and loss modulus. Activation energy associated with storage modulus arises from virgin, intact filler-filler bonds and the other from damaged filler-filler bonds which break down and reform during dynamic deformation. However, these energies still do not reach by far the level of typical chemical processes. But as the deformations involved in these Payne measurements are more representative of what happens in real wet traction or skidding of tires, it demonstrates that the value of low deformation master curves is only limited from the perspective of predicting these phenomena on basis of laboratory testing.

### **ACKNOWLEDGEMENT**

We would like to thank Apollo Vredestein for their support and the permission to present this paper. We also would like to thank Dr. Manfred Klüppel of the Deutsches Institut für Kautschuktechnologie, Hanover, Germany for fruitful discussions. We also acknowledge Jan van Kranenburg and Kuno Dijkhuis of Elastomer Research and Testing, Deventer, the Netherlands for their stimulating discussions. The financial support within the GO program (EFRO 2007-2013) from Gelderland-Overijssel is also greatly acknowledged.

### **BIBLIOGRAPHY**

- 1 M.J. Wang and Y. Kutsovsky, RUBBER CHEM. TECHNOL. **81**, 552 (2008).
- 2 K. A. Grosch, RUBBER CHEM. TECHNOL. **80**, 379 (2007).
- 3 A. G. Veith, RUBBER CHEM. TECHNOL. **69**, 654 (1996).
- 4 M. Nahmias and A. Serra, *Rubber World*. **216**, 38 (1997).

- 5 S. Kawakami, H. Hirakawa and M. Misawa, *Int. Poly. Sci. Tech.* **16**, 41(1989).
- 6 A. G. Veith, *RUBBER CHEM. TECHNOL.* **69**, 654 (1996).
- 7 X. D. Pan, *J. Phys. D: Appl. Phys.* **40**, 4657 (2007).
- 8 G. Heinrich, *Kautsch. Gummi Kunstst.* **45**, 173 (1992).
- 9 G. Heinrich, *Progr. Colloid Polym. Sci.* **90**,16 (1992).
- 10 G. Heinrich and H.B. Dumlér, *RUBBER CHEM. TECHNOL.* **71**, 53 (1998).
- 11 M.L. Williams, R.F. Landel and J.D. Ferry, *J. Am. Chem. Soc.* **77**, 3701 (1955).
- 12 J. D. Ferry, "Viscoelastic Properties of Polymers", 2nd edition, chapter 11, John Wiley & Sons, New York, 1969.
- 13 A.K. Doolittle and D.B. Doolittle, *J. Appl. Phys.* **28**, 901(1957).
- 14 M. Klüppel, *J. Phys. Condens. Matter.* **21**,1 (2009).
- 15 J. Fritzsche and M. Klüppel, *J. Phys. Condens. Matter.* **23**,1 (2011).
- 16 V. Herrmann and W. Niedermeier, *Kautsch. Gummi Kunstst.* **63**, 559 (2010).
- 17 L. Mullins, *RUBBER CHEM. TECHNOL.* **21**, 281 (1948).
- 18 F. Bueche, *J. Appl. Poly. Sci.* **5**, 271 (1961).
- 19 J. A. C. Harwood, L. Mullins and A. R. Payne, *J. Appl. Polym. Sci.* **9**, 3011 (1965).
- 20 A.R. Payne, *J. Appl. Poly. Sci.* **6**, 57 (1962).
- 21 J. Fröhlich, W. Niedermeier and H.D. Luginsland, *Composites Part A: appl. Sci. Manufacturing* **36**, 449 (2005).
- 22 M. J. Wang, Paper presented at a meeting of the Rubber Division , American Chemical Society, Indianapolis, Indiana, May 5-8 (1998).
- 23 A. Le Gal, X. Yang and M. Klüppel, *J. Chem. Phys.* **123**, 1 (2005).
- 24 M. Wang, *RUBBER CHEM. TECHNOL.* **71**, 520 (1998).

- 25 J. Berriot, H. Montes, F. Lequeux, D. Long and P. Sotta, *Macromolecules* **35**, 9756 (2002).
- 26 L. Guy, S. Daudey, P. Cochet and Y. Bomal, *Kautsch. Gummi Kunstst.* **62**, 383 (2009).
- 27 G. Heinrich and M. Klüppel, *Kautsch. Gummi Kunstst.* **57**, 452 (2004).
- 28 R. Kronig, *J. opt. Soc. Amer.* **12**, 547(1926)
- 29 H.A. Kramers, Ai Congr. Int. dei Fisici. Como (1927), p545.
- 30 H. C. Booij and G. P. J. M. Thoone, *Rheol. Acta* **21**, 15 (1982).
- 31 M. Wang, RUBBER CHEM. TECHNOL. **72**, 430 (1999).
- 32 L. Ladouce and Y. Bomal, ACS, Rubber division, Paper No. 33, Dallas, April 4-6 (2000).
- 33 L. Guy, Y. Bomal, L. Ladouce-Stenlandre and P. Cochet, *Kautsch. Gummi. Kunstst.* **58**, 43 (2005).
- 34 A. Le Gal, L. Guy, G. Orange, Y. Bomal and M. Klüppel, *Wear* **264**, 606 (2007)
- 35 B. N. J. Persson, *J. Chem. Phys.* **115**, 3840 (2001).
- 36 S. Westermann, F. Petry, R. Bpes and G. Thielen, *Kautsch. Gummi Kunstst.* **57**, 645 (2004).

Table I  
Rubber compound compositions (in phr)

Ingredient	Supplier	Sample Code		
		37S6	37S7	37S8
<b>S-SBR</b>		96.3	96.3	96.3
<b>BR</b>		30	30	30
<b>Silica</b>		60	70	80
<b>TESPT<sup>a</sup></b>	Evonik Degussa GmbH	5.2	6.1	7
<b>TDAE<sup>b</sup></b>	BP Belgium	6.7	6.7	6.7
<b>Zinc oxide</b>	Sigma Aldrich	2.5	2.5	2.5
<b>Stearic acid</b>	Sigma Aldrich	2.5	2.5	2.5
<b>6PPD<sup>c</sup></b>	Flexsys	2	2	2
<b>TMQ<sup>d</sup></b>	Flexsys	2	2	2
<b>Sulfur</b>	Sigma Aldrich	1.4	1.4	1.4
<b>TBBS<sup>e</sup></b>	Flexsys	1.7	1.7	1.7
<b>DPG<sup>f</sup></b>	Flexsys	2	2	2

<sup>a</sup> Coupling agent bis(triethoxysilylpropyl) tetrasulfide

<sup>b</sup> Treated distillate aromatic extract oil, ENERTHENE 1849 F

<sup>c</sup> Antiozonant N-phenyl-N'-1,3-dimethylbutyl-p-phenylenediamine

<sup>d</sup> Antioxidant 2,2,4- trimethyl-1,2-di-hydroquinoline

<sup>e</sup> Accelerator N-tert-butylbenzothiazole-2-sulphenamide

<sup>f</sup> Accelerator diphenyl guanidine

Table II  
 Activation energies derived from vertical shift factors and strain sweep measurements for both  
 G' and G''

	Vertical shift factor		Strain sweep		R <sup>2</sup> (%) (G'/G'')
	Ea (kJ/mol) from G'	Ea (kJ/mol) from G''	Ea (kJ/mol) from G'	Ea (kJ/mol) from G''	
<b>37S6</b>	3.3	3.2	14.9	23.4	93/94
<b>37S7</b>	5.4	5	17.6	29.9	96/97
<b>37S8</b>	8	12.1	21	33.5	95/96

## FIGURE CAPTIONS

FIG. 1. - Storage modulus data for compound 37S7 derived from frequency sweep measurements performed at different temperatures between -20 °C and 80 °C in steps of five degrees at a dynamic strain of 0.1%.

FIG. 2. - Storage modulus for 37S7 after horizontal shifting along the frequency axis,  $T_{ref} = 0$  °C.

FIG. 3.- Storage modulus master curve for 37S7,  $T_{ref} = 0$  °C.

FIG. 4. - Storage modulus master curve for the different compounds.

FIG. 5. - Loss modulus master curve for the different compounds.

FIG. 6. - Loss tangent master curve for the different compounds.

FIG. 7. - Vertical shift factor from  $G'$  vs.  $1/T$  at temperatures higher than  $T_{ref}$ .

FIG. 8. - Variation of storage modulus with strain at different temperatures from 60 to 80 °C for compound 37S8.

FIG. 9. - Variation of loss modulus with strain at different temperatures from 60 to 80 °C for compound 37S8.

FIG. 10. - Effect of filler loading on the change of the storage modulus with strain at 60 °C.

FIG. 11. - Logarithmic magnitude of storage modulus Payne effect as a function of reciprocal temperature  $1/T$  for compound 37S8.

FIG. 12. - Activation energies derived from the Payne effect and vertical shift factor for both  $G'$  and  $G''$  versus silica filler loading.